Two-dimensional vascularized liver organoid on extracellular matrix with defined stiffness for modeling fibrotic and normal tissues

Lei Ma[1], Lin Yin[1], Hai Zhu[2], Jing Li[1]
and Dong Wang[1] (iD)

Abstract

Antifibrotic drug screening requires evaluating the inhibitory effects of drug candidates on fibrotic cells while minimizing any adverse effects on normal cells. It is challenging to create organ-specific vascularized organoids that accurately model fibrotic and normal tissues for drug screening. Our previous studies have established methods for culturing primary microvessels and epithelial cells from adult tissues. In this proof-of-concept study, we used rats as a model organism to create a two-dimensional vascularized liver organoid model that comprised primary microvessels, epithelia, and stellate cells from adult livers. To provide appropriate substrates for cell culture, we engineered ECMs with defined stiffness to mimic the different stages of fibrotic tissues and normal tissues. We examined the effects of two TGFβ signaling inhibitors, A83-01 and pirfenidone, on the vascularized liver organoids on the stiff and soft ECMs. We found that A83-01 inhibited fibrotic markers while promoting epithelial genes of hepatocytes and cholangiocytes. However, it inhibited microvascular genes on soft ECM, indicating a detrimental effect on normal tissues. Furthermore, A83-01 significantly promoted the expression of markers of stem cells and cancers, increasing the potential risk of it being a carcinogen. In contrast, pirfenidone, an FDA-approved compound for antifibrotic treatments, did not significantly affect all the genes examined on soft ECM. Although pirfenidone had minor effects on most genes, it did reduce the expression of collagens, the major components of fibrotic tissues. These results explain why pirfenidone can slow fibrosis progression with minor side effects in clinical trials. In conclusion, our study presents a method for creating vascularized liver organoids that can accurately mimic fibrotic and normal tissues for drug screening. Our findings provide valuable insights into the potential risks and benefits of using A83-01 and pirfenidone as antifibrotic drugs. This method can be applied to other organs to create organ-specific vascularized organoids for drug development.

Keywords

Liver organoid, vascularization, fibrosis, stiffness, extracellular matrix

Introduction

Fibrosis is a pathological condition that can be caused by a variety of diseases and injuries and can affect almost all the organs.[1,2] During fibrosis, myofibroblasts proliferate and expand in local tissues, which leads to the deposition of excessive extracellular matrix (ECM) and causes tissue stiffening. The stiff ECM further promotes myofibroblast activation, which drives the progression of fibrosis.[3] Lack of microvessels is another important feature of fibrosis,[4]

[1]Institute for Translational Medicine, The Affiliated Hospital of Qingdao University, Medical College, Qingdao University, Qingdao, China
[2]Department of Urology, Qingdao Municipal Hospital, Qingdao University, Qingdao, China

Corresponding author:
Dong Wang, Institute for Translational Medicine, The Affiliated Hospital of Qingdao University, Medical College, Qingdao University, 38 Dengzhou Road, Shibei District, Qingdao 266021, China.
Email: dongwang@qdu.edu.cn

which further deteriorates organ functions. All these factors collectively contribute to organ fibrosis and eventually organ failure.

Many efforts have been done to study the mechanisms of organ fibrosis. The main cell type in liver fibrosis, myofibroblasts, can originate from multiple sources, such as epithelial cells, microvessels, stellate cells, fibroblasts, and adult stem cells.[4,5] These cells can be activated by various stimuli and can differentiate into myofibroblasts through the transforming growth factor beta (TGFβ) signaling pathway, which is the master regulator of fibrosis and a potential therapeutic target.[1–3] Although animal studies have made significant achievements in developing antifibrotic treatments, few of them succeeded in clinical trials.[1,6,7] Pirfenidone is the only TGFβ inhibitor that has been approved by the FDA for treating fibrosis in recent years. However, it only slows the fibrosis progression.[6] In clinical trials, the major challenges are efficacy and toxicity, which arise due to the differences between animals and humans in physiology, pathology, and genetics. Therefore, it is essential to establish precise human cell culture platforms to evaluate the inhibitory effects of drug candidates on myofibroblasts, and, more importantly, potential negative effects on normal cells, such as parenchymal and microvascular cells.

Traditional in vitro fibrosis models are limited to using only one type of cells, such as myofibroblasts, fibroblasts, or stellate cells,[3,8] which cannot fully replicate the in vivo multicellular microenvironment. In recent years, organoids have emerged as a promising solution.[9] There have been some reports about liver organoid models for fibrosis.[10,11] Hepatic stellate cells can be cultured in three dimensions (3D) to form organoids.[12] Elbadawy et al. cocultured primary mouse hepatocytes and stellate cells in vitro to form organoids.[13] Leite et al. cocultured the hepatocyte cell line HepaRG and primary human hepatic stellate cells in 3D to make liver organoids.[14] Coll et al. generated hepatic stellate cells from pluripotent stem cells and cocultured them with HepaRG cells to form organoids for fibrosis study.[15] Ouchi et al. further developed methods for generating hepatocyte like cells, stellate like cells, and Kupffer like cells from pluripotent stem cells.[16] However, incorporating microvessels into the liver organoids remains a challenge. While there are reports about vascularized organoids generated by the induction of pluripotent stem cells,[17] it is still challenging to create vascularized organoids containing organ-specific microvessels and parenchymal cells from pluripotent stem cells.

Primary cells that are isolated from adult organs are an ideal source for creating organ-specific vascularized organoids. Our previous studies have established methods for culturing epithelial cells,[18,19] microvessels,[20] and vascular stem cells[4] from adult tissues. We also engineered an extracellular matrix with defined stiffness to model fibrotic tissues.[21] In this proof-of-concept study, we aimed to establish a two-dimensional (2D) vascularized liver organoid model using rats as the model organism. This model can serve as a drug screening platform for liver fibrosis therapies. By using this model, researchers can accurately and efficiently test the effects of potential drug candidates on multiple types of cells in both fibrotic and normal tissues.

Materials and methods

Preparation of ECM substrates

The ECM substrates used in this study were mainly composed of collagen I and IV. We derived the ECM solution from decellularized porcine kidneys through pepsin digestion, as described in our earlier study.[22] The ECM solution was added to culture dishes and dried at 37°C in a sterile container to form ECM membranes. By adjusting the ECM density ($\mu g/mm^2$) on the culture dish, we were able to produce ECMs with Young's moduli of approximately 20, 6, and 1 kPa, as determined by atomic force microscopy in our previous study.[21] The culture dishes made of polystyrene had a Young's modulus of approximately 3 GPa. We incubated the culture dishes with 0.1 mg/mL ECM solution for 1 h and washed them with PBS before seeding cells.

Isolation of primary cells from adult rat livers

All animal procedures were carried out in accordance with the Ministry of Science and Technology Guide and approved by the Animal Care and Use Committee of Qingdao University. The Sprague Dawley (SD) rats of 8–10 weeks were euthanized by an overdose of isoflurane (RWD, cat#R510-22-10). The livers were harvested and cut into 2 mm pieces and then digested in DMEM (Invitrogen, Cat#12800017) supplemented with 2 mg/mL collagenase I (Worthington, Cat#LS004196) and 5 μM Y27632 (Selleck, Cat#S1049).

Primary liver cells were collected during cyclic digestion.[20,21] The cell suspension was filtered through a 150 μm strainer every 20 min, and the tissues collected on the strainer were subjected to another round of digestion until all the tissue pieces were digested. The final cell suspension was filtered through a 30 μm strainer to eliminate red blood cells and single cells. The cells that remained on the 30 μm strainer were collected for experiments.

Culture of primary liver cells

Primary liver cells were cultured on the ECMs with different stiffness in a custom-made medium. The medium was DMEM/F12 supplemented with N2 (Gibco, Cat#17502048), B27 (Gibco, Cat#17504044), 2% fetal bovine serum (FBS, Gibco, Cat#10091148), 100 U/mL penicillin and 100 μg/mL streptomycin (Gibco, Cat#15140122). Control medium

was supplemented with 2 µM Chir99021 (Selleck, Cat#S2924), 5 µM Y27632 (Selleck, Cat#S1049), and 10 ng/mL VEGF (Peprotech, Cat#100-20), and experimental medium was supplemented with 0.2 µM A83-01 or 0.2 mg/mL pirfenidone (Selleck, Cat#S2907). The cells were cultured in an incubator at 37°C, 5% CO_2, and 95% humidity.

Total RNA extraction

Total RNA was extracted from liver cells using TRIzol™ Reagent (Invitrogen, Cat#15596026). The cells were lysed in 60 mm culture dishes using 1 mL of TRIzol™ Reagent. 200 µL of chloroform was added to the lysate and left on ice for 10 min. It was then centrifuged at 12,000 rpm 4°C for 10 min. Next, 400 µL of supernatant was transferred to a new tube and 500 µL of isopropanol was added. The mixture was centrifuged at 10,000 rpm 4°C for 10 min. The RNA precipitate was washed three times with 75% ethanol at 10,000 rpm and 4°C for 5 min by centrifugation. The RNA precipitates were air-dried for 5–10 min and subsequently dissolved in 10–50 µL of DEPC water. RNA was identified and quantified using Nano Drop and Agilent 2100 Bioanalyzer.

Quantitative PCR analysis

Sample RNA was reverse transcribed to cDNA using Evo M-MLV RT Mix with gDNA Clean for qPCR Ver.2, and qPCR experiments were performed using MonAmp™ ChemoHS qPCR Mix. Fold change in mRNA expression levels was calculated by the comparative Ct method, using the formula $2^{-\Delta\Delta Ct}$ and GAPDH as a calibrator. The primer list was attached to the Supplemental Materials.

Immunostaining

The cells were fixed in 4% paraformaldehyde (PFA) for 30 min, washed three times with PBS, permeabilized with 1% Triton for 10 min, blocked in 5% normal donkey serum for 1 h, and incubated with primary antibodies in a blocking solution at 4°C overnight. After primary antibody incubation, the cells were washed three times in PBS and incubated with secondary antibodies in the blocking solution for 10 h at 4°C. The primary antibodies used in this study were CD31 (Affinity, Cat#AF3628), E-cadherin (Proteintech, Cat#20874-1-AP), E-cadherin (Sangon Biotech, Cat#D194898), SMA (Santa Cruz, Cat#SC32251), Desmin (Proteintech, Cat#16520-1-AP), Collagen I (Affinity, Cat#AF7001), p-ITGB1 (Affinity, Cat#AF8384), CTGF (Affinity, Cat#AF7537). Cell nuclei were stained by DAPI (4′,6-diamidino-2-phenylindole). Confocal imaging was performed on a Leica SP8 confocal microscope.

Statistical analysis

All experimental data were presented as mean ± SD of three replicates. Immunofluorescence staining results were processed using ImageJ. One-way ANOVA was performed using Graghpad Prism 8 for single-factor data and two-way ANOVA for two-factor data followed by Bonferroni post hoc test. Mann Whitney test was performed between two groups. $p < 0.05$ was considered a significant difference.

Results

2D vascularized liver organoids

After digesting the liver tissue, we filtered the cell suspension through a 30 µm strainer to remove red blood cells and debris. The remaining microvascular segments and epithelial clusters were self-organized into multiple layers within 4 days when cultured in regular dishes with Young's modulus of about 3 GPa (Figure 1(a) and (b)). Immunostaining showed that CD31^{+} microvessels grew on top of the E-cadherin^{+} epithelial layer (Figure 1(c) and (d)). There were plenty of Desmin^{+} stellate cells surrounding the microvessels (Figure 1(e)). While this 2D vascularized liver organoid does not have the typical three-dimensional spherical structure of a classical organoid, it has advantages such as the feasibility of performing immunostaining and the potential for replicating the liver's matrix in various liver diseases.

Examine the antifibrotic effect of A83-01 on 2D vascularized liver organoids on the ECM with defined stiffness mimicking fibrotic and normal microenvironments

In clinical studies, it has been found that the Young's modulus of liver tissues of advanced fibrosis is above 7 kPa, while for cirrhosis, it is higher than 13 kPa.[23,24] Normal liver tissues have a Young's modulus of about 1 kPa.[25,26] To mimic these conditions, we engineered ECM substrates with Young's moduli of approximately 20 and 6 kPa to mimic fibrotic liver tissues, as well as an ECM gel of about 1 kPa for normal liver tissues (Figure 2(a) and (b)).[21] Additionally, we also included a group of regular culture dishes with a Young's modulus of about 3 GPa for comparison. These ECM substrates were mainly composed of collagen I and IV, without any synthetic polymers, and could better mimic the ECM in vivo.[22]
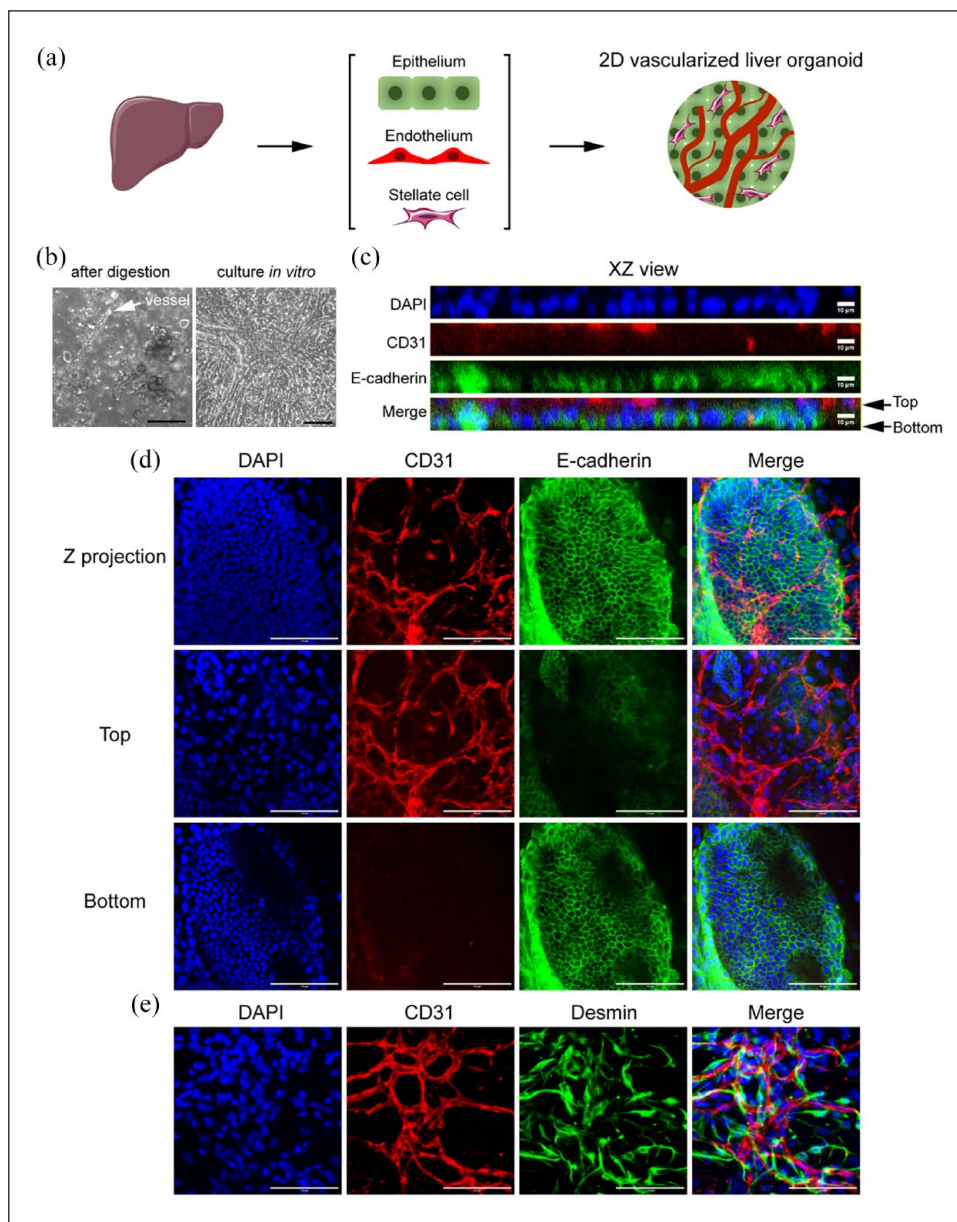
Figure 1. 2D vascularized liver organoids. (a) Workflow illustration. (b) The phase contrast images of the primary liver cells right after digestion and those cultured in vitro in regular dishes for 4 days. The white arrow pointed to a microvessel. (c–e) Immunostaining of the 2D vascularized liver organoids cultured for 4 days in vitro. The antibodies were against CD31, E-cadherin, and Desmin. DAPI stained nuclei. Scale bars, 100 μm.

We first examined two extreme conditions, including the softest (1 kPa) and the stiffest (3 GPa) ECM substrates, by immunostaining. We observed that epithelial cells lost their typical cobblestone morphology on these ECMs, as shown by disorganized E-cadherin staining and strong SMA signals, suggesting epithelial-mesenchymal transition (EMT) and differentiation into myofibroblasts (Figure 2(c)). The TGFβ signaling pathway is the master regulator of organ fibrosis and EMT. The addition of a TGFβ receptor inhibitor, A83-01, restored the epithelial cell morphology (E-cadherin staining pattern) and inhibited SMA expression on the soft 1 kPa ECM (Figure 2(c)). However, A83-01 failed to reverse the epithelial morphology and SMA expression on 3 GPa ECM (Figure 2(c)), indicating that multiple signaling pathways regulate this phenotype change at high stiffness.

The quantitative analysis using qPCR showed that A83-01 treatment significantly upregulated the expression of genes of epithelial cells (*Cdh1/E-cadherin*), hepatocytes (*Krt8*, *Krt18*, and *Alb*), and cholangiocytes (*Krt7* and *Krt19*; Figure 2(d)). All types of stiff ECMs, including 6 kPa, 20 kPa, and 3 GPa, upregulated *Cdh2* expression,
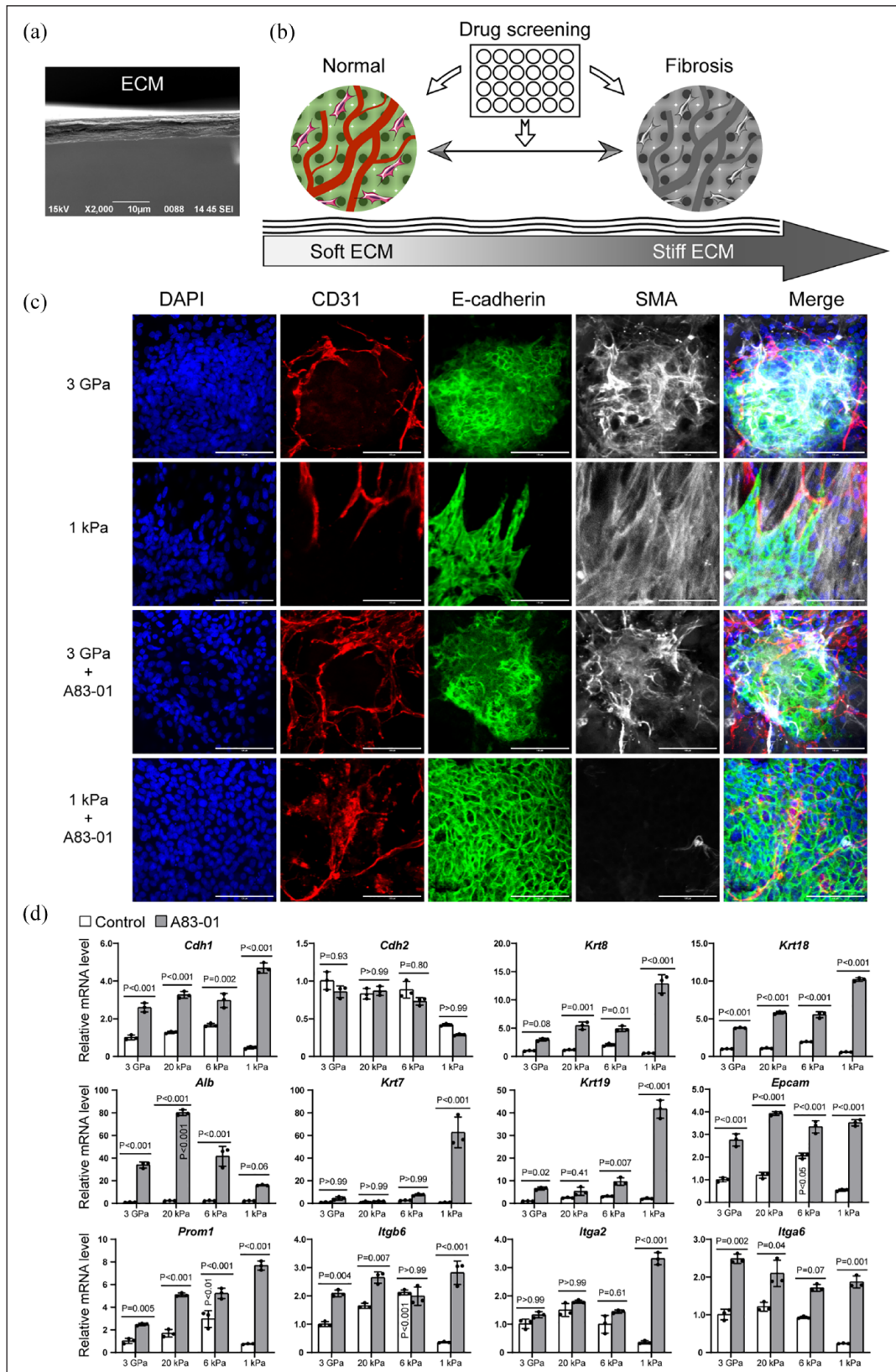
Figure 2. Drug screening using vascularized liver organoids on stiff and soft ECMs. (a) SEM image of ECM cross-section. (b) Illustration of the workflow. (c) Immunostaining of vascularized liver organoids on the ECM of 3 GPa and 1 kPa with or without A83-01. The antibodies were against CD31, E-cadherin, and SMA. DAPI stained nuclei. Scale bars, 100 μm. (d) qPCR analysis of the effect of A83-01 on vascularized liver organoids on different ECM (3 GPa, 20 kPa, 6 kPa, and 1 kPa). $N = 3$. Two-way ANOVA was performed on the data followed by Bonferroni post hoc tests. $p < 0.05$ was considered significant. The culture time was 1 week.

which is consistent with the EMT in fibrotic tissues. We found that A83-01 did not have an effect on *Cdh2* expression in any of these conditions, suggesting the involvement of multiple signaling pathways in liver EMT. The greatest increase in the expression of *Cdh1*, *Krt8*, *Krt18*, *Krt7*, and *Krt19* due to A83-01 treatment was observed on the 1 kPa ECM. Interestingly, in the A83-01 group, *Alb* expression increased with increasing ECM stiffness from 1 to 20 kPa, but then decreased on 3 GPa ECM. It is worth noting that Albumin (Alb) was reduced significantly during liver fibrosis.[27] The increase of *Alb* on the 20 kPa ECM may indicate a compensatory mechanism for the loss of *Alb* during liver fibrosis, which warrants further investigation in the future. This also suggests that engineered ECM substrates are more effective than regular culture dishes for in vitro liver fibrosis research. These results suggest that A83-01 promoted liver epithelial cell phenotype and marker expression, especially on the soft ECM of 1 kPa.

We also investigated *Epcam*, *Prom1*, *Itgb6*, *Itga2*, and *Itga6* (Figure 2(d)), which have been reported to be associated with cancers. *Epcam* and *Prom1* are known as markers of liver cancer stem cells.[28] *Itgb6* has been reported to contribute to liver fibrosis and intrahepatic cholangiocarcinoma.[29] *Itga6* has been found to promote hepatocellular carcinoma,[30,31] while *Itga2* has been linked to multiple cancers.[32–34] We found that *Epcam*, *Prom1*, and *Itgb6* had the highest expression on 6 kPa ECM, which corresponds to the early stages of liver fibrosis. Most cases of liver fibrosis eventually progress to cancers in the late stages.[35] The upregulation of these genes on 6 kPa ECM might be one of the mechanisms of premalignant factors, which warrants further study in the future.

Stellate cells are an important source of myofibroblasts during liver fibrosis.[5] Our immunostaining results showed Desmin$^+$ stellate cells around microvessels on the ECMs of 3 GPa and 1 kPa, and they exhibited strong staining for SMA (Figure 3(a)). A83-01 treatment reduced SMA expression significantly on the ECM of 1 kPa but not on 3 GPa ECM (Figure 3(a)). By qPCR analysis, we found that the stellate cell marker *Desmin* was upregulated on stiff ECMs and further elevated by A83-01 treatment (Figure 3(b)). *Pdgfrb* had higher expression on stiff ECMs but was not regulated significantly by A83-01 treatment (Figure 3(b)). Interestingly, *Lrat* had the highest expression on 20 and 6 kPa ECMs, which corresponds to pathological fibrotic liver tissues. Overall, most fibrotic markers were upregulated on stiff ECMs, such as *Acta2* (*Sma*), *Col1a1*, *Col3a1*, *Fn1*, *Postn*, *Fap*, *Vim*, and *Lox* (Figure 3(b)). *Fn1*, *Postn*, *Fap*, and *Lox* had the highest expression on the ECMs with pathological stiffness of 20 and/or 6 kPa ECM, demonstrating the effectiveness of our engineered ECM substrates in mimicking liver fibrosis.

A83-01 treatment reduced the expression of most fibrotic genes on stiff ECMs, except *Vim* and *Lox*. The decrease of some genes on the soft ECM of 1 kPa was not significant possibly because of the small values (Figure 3(b)). Immunostaining results showed that COL1 was reduced by A83-01, particularly on the ECM of 1 kPa (Figure 4). These results suggest that A83-01 inhibited fibrosis effectively.

Complex roles of A83-01 on the endothelial cells

Effective antifibrotic therapies need to not only inhibit fibrosis but also restore microvessels. Therefore, we investigated the impact of A83-01 on critical microvascular genes (Figure 5). We found that the angiogenic gene *Apln* was significantly upregulated on stiff ECMs of 3 GPa, 20 kPa, and 6 kPa, but was downregulated on the soft ECM of 1 kPa by A83-01 (Figure 5(a)). Similarly to the results of some epithelial, stellate cell, and fibrotic genes (Figures 2(d) and 3(b)), we noticed that 3 GPa ECM had lower *Apln* expression than 20 kPa in both control and A83-01 groups. The other endothelial genes examined in this study had a higher expression on stiff ECMs in both control and A83-01 groups. The tyrosine kinase receptor *Tek* was significantly reduced on the soft 1 kPa ECM under A83-01 treatment. The trend of *Tie1* was similar to *Tek*. *Pecam1* (*Cd31*) showed a decrease on 20 kPa ECM but an increase on 6 kPa ECM under A83-01 treatment. Additionally, the expression of *Cdh5* was found to decrease on 3 GPa and 20 kPa ECMs under A83-01 treatment. Furthermore, we observed that VEGF receptors (*Flt1*, *Kdr*, and *Flt4*) were upregulated on stiff ECMs to different extents by A83-01. A83-01 insignificantly affected *Flt1*, upregulated *Kdr* on 3 GPa ECM, and promoted *Flt4* on 3 GPa and 20 kPa ECMs (Figure 5(a)). These results suggest that A83-01 has varying effects on endothelial cells in fibrotic and normal tissues. Considering the negative effects of A83-01 on *Apln*, *Tek*, and *Tie1* on 1 kPa ECM, we measured microvascular lengths on 1 kPa ECM with and without A83-01 treatment. The results revealed that A83-01 significantly reduced microvascular growth on the soft 1 kPa ECM (Figure 5(b)), suggesting its potential to harm normal liver tissues.

Integrins in vascularized liver organoids

Integrin family proteins are of critical importance in transducing signals from the ECM to the cells. In our study of vascularized liver organoids, we conducted a comprehensive qPCR analysis to examine the expression of Integrin proteins in the absence of A83-01 (Figure 6(a)). The results showed that among the subunits, Integrin β1 (*Itgb1*) exhibited the most significant upregulation in the cells of the control group that underwent fibrosis in vitro. The other subunits, namely *Itga1*, *Itga5*, *Itga11*, and *Itgav*, also showed comparatively higher expression levels than the rest (Figure 6). We further investigated these five Integrins
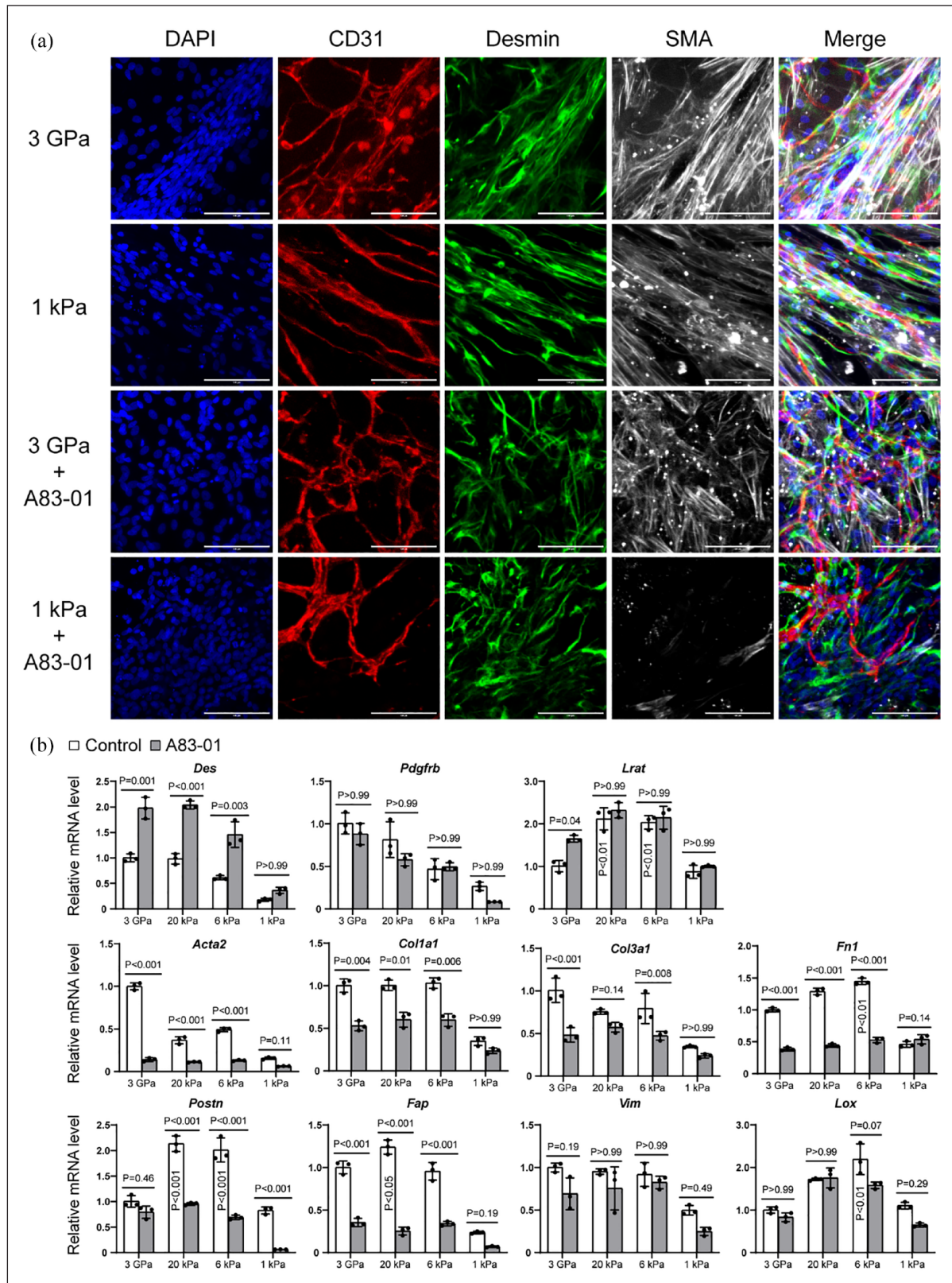
Figure 3. Stellate cell and fibrotic markers of vascularized liver organoids regulated by ECM stiffness and A83-01. (a) Immunostaining of vascularized liver organoids on the ECM of 3 GPa and 1 kPa with or without A83-01 treatment. The antibodies were against CD31, Desmin, and SMA. DAPI stained nuclei. Scale bars, 100 μm. (b) qPCR analysis of vascularized liver organoids on the ECM of 3 GPa, 20 kPa, 6 kPa, and 1 kPa, with or without A83-01. $N = 3$. Two-way ANOVA was performed on the data, followed by Bonferroni post hoc tests. $p < 0.05$ was considered significant. The culture time was 1 week.
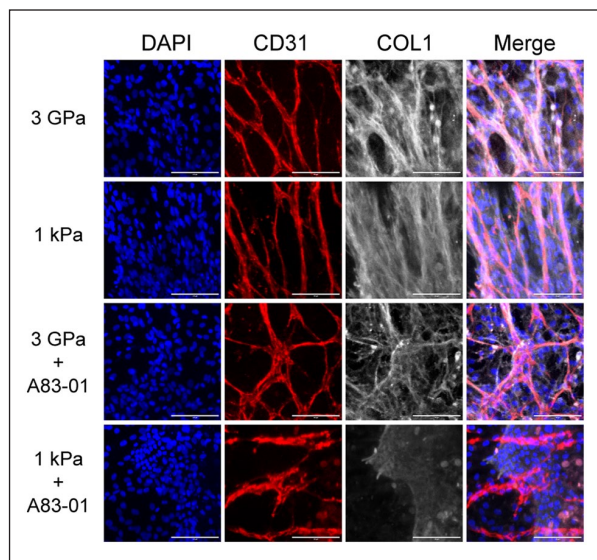
Figure 4. COL1 expression of vascularized liver organoids on different stiffness with or without A83-01. The primary vascularized liver organoids were cultured for 1 week before being immunostained by the antibodies against CD31 and COL1. DAPI stained nuclei. Scale bars, 100 μm.

in vascularized liver organoids on ECMs of different stiffness with or without A83-01. We found that stiff ECMs of 3 GPa, 20 kPa, and 6 kPa had higher expression of the five Integrins than 1 kPa ECM, indicating the activation of these genes during fibrosis. However, all the five Integrins were downregulated on stiff ECMs by A83-01, except that *Itgav*'s changes were not significant. It is worth noting that A83-01 did not influence these five Integrins on soft ECM of 1 kPa (Figure 6(a)).

Given that *Itgb1* was the most abundant subunit, we performed immunostaining on vascularized liver organoids to investigate its subcellular localization. Our results showed that the phosphorylated ITGB1 (p-ITGB1; Y783) was mainly located in the endothelial and epithelial cells, but not in stellate cells, on the 3 GPa ECM in the control medium, which promoted fibrosis (Figure 6(b)). This result is in agreement with our previous study on subcutaneous microvessels, where endothelial cell p-ITGB1 (Y783) mediated mechanotransduction from ECM to endothelial cells.[21] In the liver, both endothelial cells and epithelial cells are potential mechanosensors during fibrosis.

Paracrine growth factors during fibrosis

To explore the potential downstream paracrine growth factors of endothelial cells and epithelial cells, we conducted qPCR analysis of vascularized liver organoids on 3 GPa ECM in the control medium. Among the four major fibrotic growth factors, including *Ctgf*(*Ccn2*), *Tgfb1*, *Tgfb2*, and *Tgfb3*, *Ctgf* was the most expressed one (Figure 7(a)). Our immunostaining results showed that both endothelial and epithelial cells were the primary sources of CTGF (Figure

7(b)). A83-01 significantly reduced *Ctgf* on 3 GPa ECM while increasing it on 1 kPa ECM (Figure 7(a)). The effects of A83-01 on *Tgfb1*, *Tgfb2*, and *Tgfb3* were also complex. A83-01 reduced *Tgfb1* on 20 kPa ECM but not on others, reduced *Tgfb2* on 3 GPa but increased it on 1 kPa, and reduced *Tgfb3* on 3 GPa but increased it on 20 kPa ECM (Figure 7(a)). These results suggest that A83-01 regulates these fibrotic growth factors depending on the ECM stiffness of the local microenvironment.

Our study has shown that A83-01 can reduce fibrotic genes, elevate epithelial genes, and increase endothelial genes on stiff ECM but reduce them on soft ECM. We have also observed that it reduced paracrine fibrotic growth factor genes on stiff ECM but promoted them on soft ECM. Furthermore, it can promote the expression of genes related to tumor formation. While the TGFβ signaling pathway participates in many biological processes, it is difficult to target them solely as an antifibrotic target without affecting other processes. Our findings are significant as they provide crucial insights into the use of A83-01 as a potential antifibrotic drug. There have been clinical trials for targeting the downstream factors, such as CTGF and TGFβ members. Among these drug candidates, a TGFβ inhibitor, pirfenidone, has been approved by the FDA for treating idiopathic pulmonary fibrosis. We next examined the effects of pirfenidone on the vascularized liver organoids.

The effects of pirfenidone on vascularized liver organoids

We found that pirfenidone did not significantly affect the expression of all genes examined on 1 kPa ECM, indicating that it may not impact normal tissues while inhibiting fibrosis in fibrotic regions of the liver (Figure 8). However, it had complex effects on these genes on the stiff ECMs of 3 GPa, 20 kPa, and 6 kPa, representing different stages of liver fibrosis (Figure 8).

1. Epithelia: Pirfenidone did not significantly regulate *Cdh1* or *Krt8*, but it did upregulate *Alb* expression in all three stiff conditions (Figure 8(a)). It increased *Cdh2* on 3 GPa and 6 kPa ECMs, increased *Krt18* on 3 GPa ECM but reduced it on 20 kPa ECM. Pirfenidone reduced *Krt19* on 20 kPa ECM, but not in other groups (Figure 8(a)). These findings suggest that pirfenidone's effect on liver epithelial cells depends on ECM stiffness, which is correlated with the stage of fibrotic diseases.
2. Stellate cells: Pirfenidone did not significantly affect the expression of stellate cell markers in all conditions of this study (Figure 8(b)).
3. Myofibroblasts: Pirfenidone did not significantly affect *Acta2*, *Postn*, or *Vim* in all conditions, and even increased *Fn1* on 3 GPa and 6 kPa, *Fap* on 6 kPa, and *Lox* on 3 GPa and 6 kPa ECMs. However, pirfenidone reduced *Col1a1* on 6 kPa ECM, and
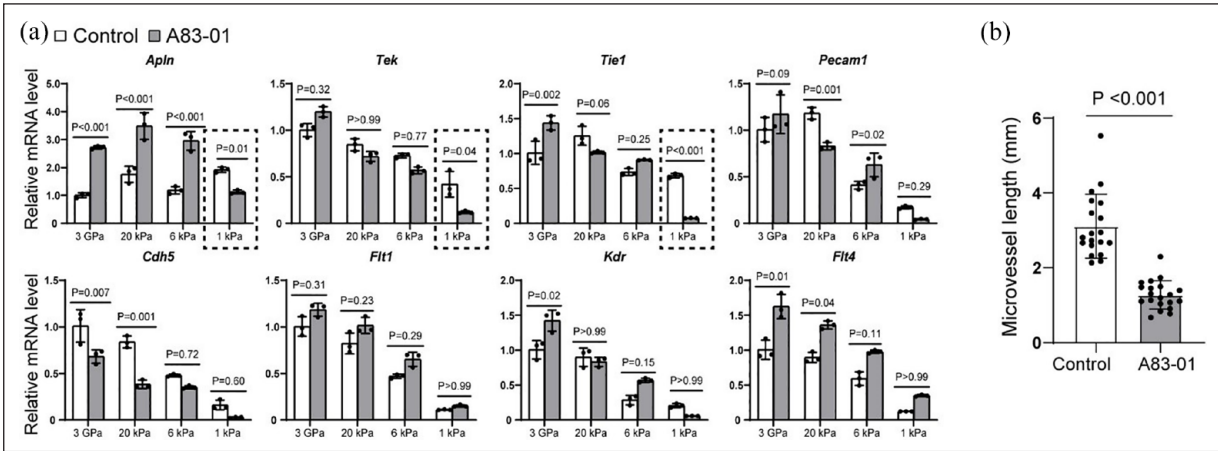
Figure 5. Endothelial cells regulated by ECM stiffness and A83-01. (a) The primary vascularized liver organoids were cultured on the ECM of different stiffness with or without A83-01 for 1 week before harvest for qPCR analysis. $N = 3$. Two-way ANOVA was performed on the data, followed by Bonferroni post hoc tests. (b) The lengths of microvessels on 1 kPa ECM in control medium and A83-01 medium. Mann Whitney test was performed between the two groups. $p < 0.05$ was considered significant.
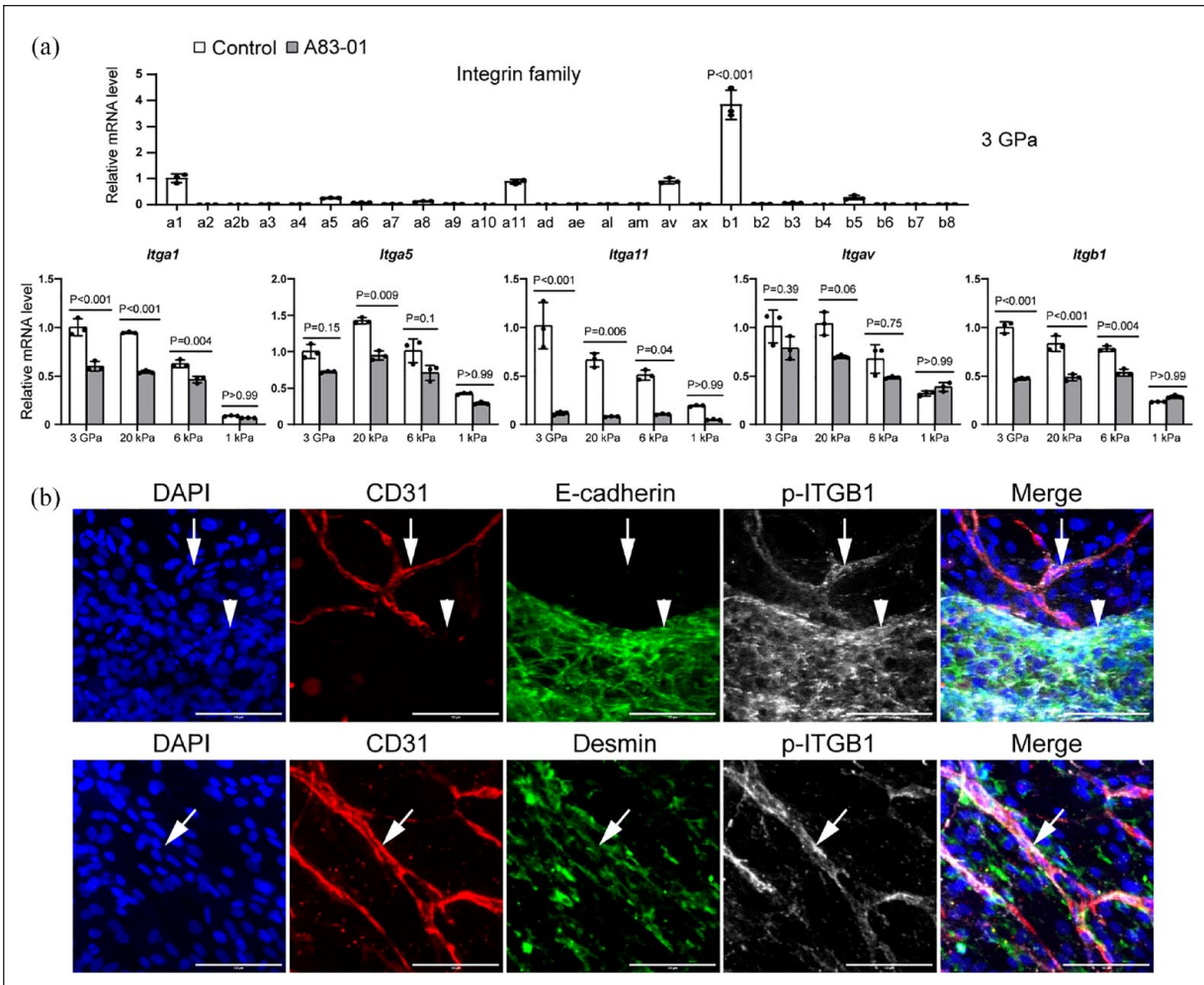

Figure 6. Integrins in vascularized liver organoids. (a) The qPCR analysis of vascularized liver organoids on the ECM of different stiffness. $N = 3$. One-way or two-way ANOVA was performed on the data, followed by Bonferroni post hoc tests. $p < 0.05$ was considered significant. (b) Immunostaining of vascularized liver organoids cultured on 3 GPa ECM in the control medium by the antibodies against CD31, E-cadherin, and p-ITGB1 (Y783). DAPI stained nuclei. Arrows pointed to CD31^{+} p-ITGB1^{+} microvascular endothelial cells. Arrowheads pointed to E-cadherin^{+} p-ITGB1^{+} epithelial cells. Scale bars, 100 μm. The cell culture time was 1 week.
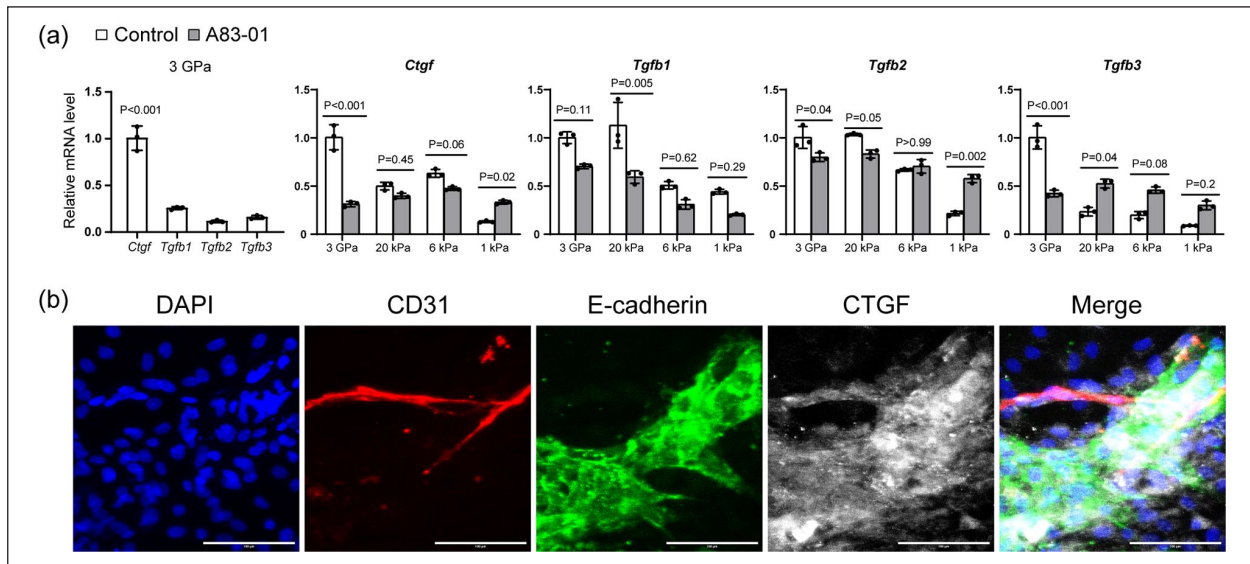
Figure 7. Paracrine growth factors during fibrosis. (a) The qPCR analysis of vascularized liver organoids on the ECM of different stiffness with or without A83-01. $N = 3$. One-way or two-way ANOVA was performed on the data, followed by Bonferroni post hoc tests. $p < 0.05$ was considered significant. (b) Immunostaining of vascularized organoids cultured on 3 GPa ECM in the control medium for 1 week. The antibodies were against CD31, E-cadherin, and CTGF. DAPI stained nuclei. Scale bars, 100 μm.

reduced *Col3a1* on all stiff ECMs, indicating that it can inhibit liver fibrosis, especially in the early stages of liver fibrosis (Figure 8(c)).

4. Endothelia: Pirfenidone did not affect most endothelial genes significantly, but it did increase *Pecam1* on all the stiff ECMs and increased *Kdr* on 20 kPa ECM (Figure 8(d)).
5. Fibrotic integrins: Pirfenidone increased *Itga1* on 3 GPa and 6 kPa ECMs, but reduced *Itga11* on 20 kPa and 6 kPa ECMs. It had no significant effects on *Itga5*, *Itgav*, or *Itgb1* (Figure 8(e)).
6. Paracrine factors: Pirfenidone increased *Ctgf* (*Ccn2*) on 3 GPa ECM but reduced it on 20 kPa ECM, increased *Tgfb1* on all stiff ECMs, increased *Tgfb2* on 3 GPa and 6 kPa ECMs, and reduced *Tgfb3* on 20 kPa ECM (Figure 8(f)).
7. Stem cells and cancers: Pirfenidone increased *Epcam* and *Prom1* expression on 6 kPa ECM, reduced *Itgb6* on all the stiff ECMs, reduced *Itga2* on 3 GPa and 20 kPa, and had no significant effect on *Itga6* in all conditions (Figure 8(g)). These findings suggest that pirfenidone can upregulate *Epcam* and *Prom1* in the early stage of liver fibrosis, indicating the potential risk of cancer formation.

Discussion

Creating vascularized organoids is a complex task. While pluripotent stem cells have been used to generate microvessels, parenchymal cells, and mesenchymal cells for developing vascularized organoids,[36,37] obtaining organ-specific microvessels and parenchymal cells from these cells is

quite challenging. This is why primary cells from adult tissues are considered the ideal sources for making vascularized organoids. Our research group has been working on in vitro culture models for adult epithelial stem cells,[18,19] microvessels,[20,22] and vascular stem cells.[4,38] In this proof-of-concept study, we have presented a method for culturing vascularized liver organoids from adult livers. The vascularized liver organoids contained primary liver epithelial cells, including hepatocytes and cholangiocytes, microvessels, and stellate cells, presenting a multicellular drug-screening platform for liver diseases.

There have been several methods for inducing liver fibrosis in vitro, such as the addition of Allyl alcohol,[14] Methotrexate,[14] free fatty acid,[16] TGFβ,[15] or thioacetamide.[15] Our study manufactured an ECM with defined stiffness that mimics the different stages of liver fibrosis.[21] To induce liver fibrosis, we cultured vascularized liver organoids on stiff ECM, leading to epithelial cells undergoing EMT and stellate cells differentiating into myofibroblasts, expressing high levels of SMA and collagens. There were also microvessels growing in the coculture system. Our engineered ECM provides a well-defined and reliable fibrotic microenvironment, making it a proper in vitro liver model for investigating multiple types of cells, in both normal tissues and fibrotic tissues at different stages.

The TGFβ signaling pathway is the master regulator of fibrosis and a promising target for therapeutic intervention.[1–3] Despite numerous clinical trials targeting this pathway, however, very few have been successful.[1–3] Pirfenidone is the only antifibrotic drug approved by the FDA in recent years that can inhibit TGFβ signaling, although its mechanism of action remains unclear.[39] In our
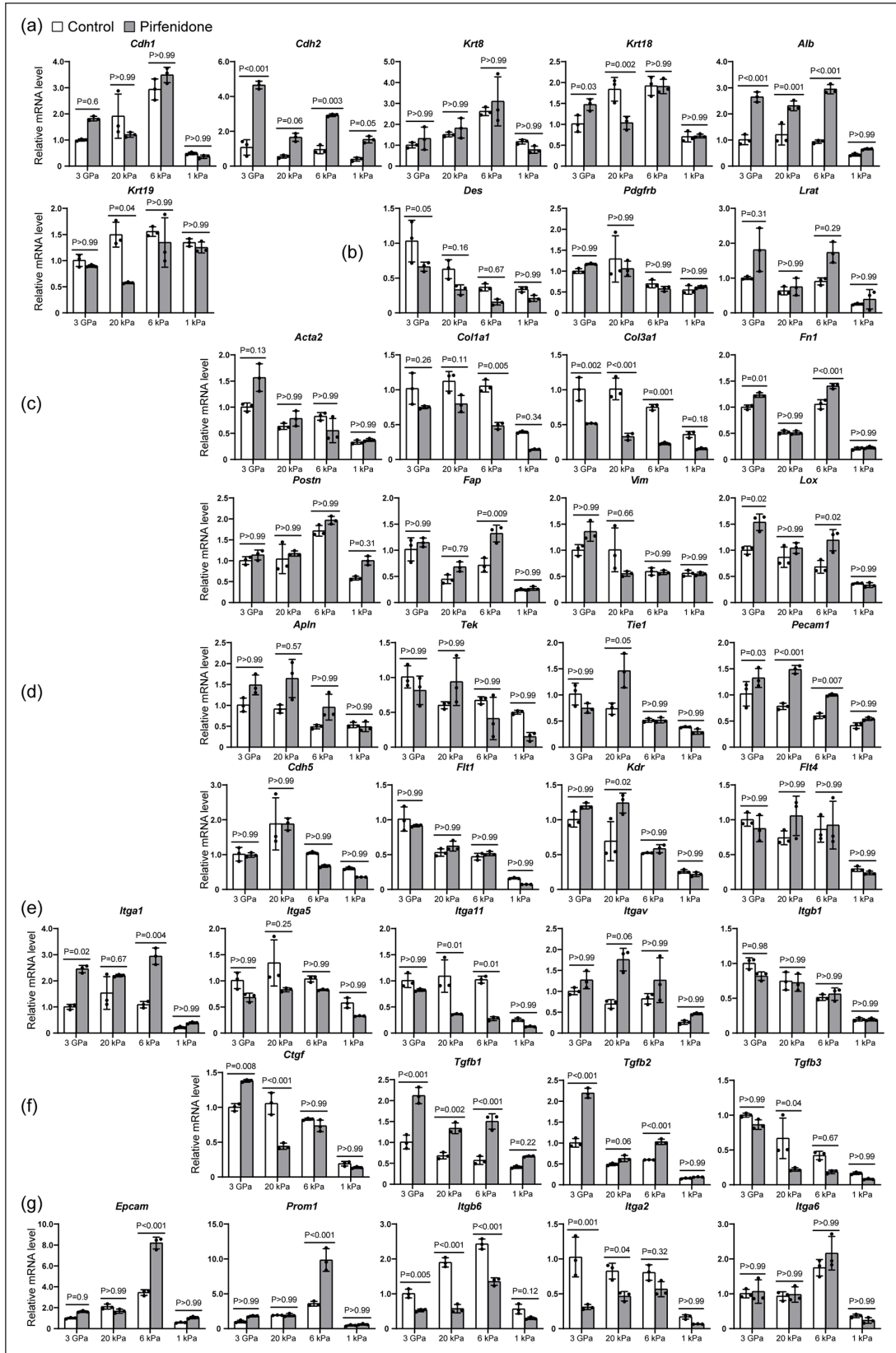
Figure 8. The effects of pirfenidone on vascularized liver organoids on stiff and soft ECM. The qPCR analysis of vascularized liver organoids cultured on the ECM of different stiffness with or without pirfenidone for 1 week. *N* = 3. Two-way ANOVA was performed on the data, followed by Bonferroni post hoc tests. *p* < 0.05 was considered significant: (a) epithelia, (b) stellate cells, (c) myofibroblasts, (d) endothelia, (e) fibrotic integrins, (f) paracrine factors, and (g) stem cells and cancers.

study, we investigated the efficacy of two TGFβ signaling inhibitors: A83-01 and pirfenidone. Our results showed that A83-01, an ALK4/5/7 inhibitor, significantly inhibited myofibroblast genes while promoting liver epithelial genes of hepatocytes and cholangiocytes. However, A83-01 inhibited microvascular genes on soft ECM of 1 kPa, suggesting that it may have negative effects on the microvessels in healthy tissues. Moreover, A83-01 significantly increased the expression of genes associated with cancers, implying its potential as a carcinogen.

In contrast, we found that pirfenidone did not have a significant effect on all the genes of vascularized liver organoids examined on the soft ECM of 1 kPa. These results suggest that it may not be toxic to the healthy liver tissues. Although pirfenidone did not have a strong inhibitory role in most fibrotic genes, it did inhibit collagen genes, including *Col1a1* and *Col3a1*, which encode the major components of fibrotic ECM. Therefore, it can be concluded that pirfenidone can slow fibrotic progression with minor side effects and was finally approved by the FDA. It is worth noting that our study found that pirfenidone significantly promoted *Epcam* and *Prom1* expression on the ECM of 6 kPa. This indicates a potential risk of tumor formation in the local areas at the early stage of liver fibrosis. Overall, our study provides new insights into the efficacy and safety of TGFβ signaling inhibitors, which could pave the way for improved therapeutic strategies for fibrosis.

The Integrin family proteins play a crucial role in transducing physical signals from the ECM to cells.[40] Our previous study has identified ITGB1 as the major subunit involved in microvascular mechanotransduction.[21] Stiff ECM can induce the phosphorylation of ITGB1 (p-ITGB1) of endothelial cells, which were activated to secret paracrine factors including CTGF and TGFβ1-3 to induce pericyte differentiation into myofibroblasts.[21] In this study, we have also found that p-ITGB1 and CTGF were located in both endothelial and epithelial cells, indicating their critical role in regulating liver fibrosis. Although some clinical trials have tested antifibrotic treatments targeting integrins[41] and CTGF,[42] there have been no positive reports yet. Further investigation is necessary to understand the regulatory mechanisms of endothelial and epithelial cells in liver fibrosis.

Fibrosis is a complex process that involves multiple types of cells and signaling pathways.[1–3] Our study has demonstrated that antifibrotic treatments must consider multiple cell types in the organs. It is crucial to thoroughly assess the antifibrotic efficacy in fibrotic tissues while also taking into account the potential negative effects on healthy cells. Our study has shown that the effects of TGFβ signaling inhibitors on vascularized liver organoids are dependent on the stiffness of the ECM. This highlights the importance of developing drug strategies that target different stages of tissue fibrosis. Further study is warranted to investigate the mechanisms underlying ECM stiffness regulation of antifibrotic effects.

Our study has some limitations that need to be addressed in future research. Firstly, the cells of vascularized liver organoids were grown in a 2D culture, which may not accurately reflect the conditions in a 3D microenvironment. Our future work will focus on developing 3D vascularized liver organoids with a defined stiffness to better mimic the in vivo microenvironment. Secondly, the cells were in a static culture, which means that blood flow shear stress was not considered. Blood flow plays a crucial role in regulating microvessels. Therefore, future research should incorporate blood flow into the organoid system to better simulate the in vivo conditions. Moreover, there were no immune cells in the vascularized liver organoids, which should be addressed in future studies. Finally, this proof-of-concept study utilized animal cells, which had limited implications in translational medicine. It is necessary to culture primary human vascularized liver organoids in future studies.

Conclusion

We have developed an adult vascularized liver organoid model to evaluate the effects of drug candidates on liver epithelial cells, including hepatocytes and cholangiocytes, microvessels, and stellate cells, in both normal tissues and fibrotic tissues at different stages. We tested two TGFβ signaling inhibitors, A83-01 and the FDA-approved antifibrotic drug pirfenidone. Our findings showed that A83-01 inhibited fibrotic genes but also inhibited microvessels and promoted cancer-related genes in normal healthy tissues, indicating severe side effects. On the other hand, pirfenidone inhibited the expression of collagens and did not affect the cells in normal tissues, explaining its clinical performance. Our 2D vascularized liver organoid model provides a more comprehensive assessment of drug candidates and has the potential to be extended to other organs for drug development.

Author contributions

DW designed the experiments. LM performed primary cell isolation, immunostaining, and confocal imaging. LM and LY performed qPCR analysis. LM fabricated the ECMs for cell culture. LM, JL, HZ, and DW analyzed the data. DW and LM wrote the manuscript.

Availability of data and materials

The data required to reproduce these findings can be made available upon reasonable request.

Declaration of conflicting interests

The author(s) declared no potential conflicts of interest with respect to the research, authorship, and/or publication of this article.

Ethical approval

The animal procedure was conducted according to the Ministry of Science and Technology guide for laboratory animal care and use and approved by the animal care and use committee of Qingdao University.

ORCID iD

Dong Wang https://orcid.org/0000-0003-3489-915X

Supplemental material

Supplemental material for this article is available online.

References

1. Henderson NC, Rieder F and Wynn TA. Fibrosis: from mechanisms to medicines. *Nature* 2020; 587: 555–566.
2. Rockey DC, Bell PD and Hill JA. Fibrosis—a common pathway to organ injury and failure. *N Engl J Med* 2015; 372: 1138–1149.
3. Long Y, Niu Y, Liang K, et al. Mechanical communication in fibrosis progression. *Trends Cell Biol* 2022; 32: 70–90.
4. Wang D, Wang A, Wu F, et al. Sox10+ adult stem cells contribute to biomaterial encapsulation and microvascularization. *Sci Rep* 2017; 7: 40295.
5. Kim HY, Sakane S, Eguileor A, et al. The origin and fate of liver myofibroblasts. *Cell Mol Gastroenterol Hepatol* 2024; 17: 93–106.
6. Castelli G, Cocconcelli E, Bernardinello N, et al. Idiopathic pulmonary fibrosis: 8 years on after nintedanib and pirfenidone approval—what is on the horizon? *Curr Pulmonol Rep* 2023; 12: 113–124.
7. Odagiri N, Matsubara T, Sato-Matsubara M, et al. Antifibrotic treatments for chronic liver diseases: the present and the future. *Clin Mol Hepatol* 2021; 27: 413–424.
8. Lee YS and Seki E. In vivo and in vitro models to study liver fibrosis: mechanisms and limitations. *Cell Mol Gastroenterol Hepatol* 2023; 16: 355–367.
9. Takebe T and Wells JM. Organoids by design. *Science* 2019; 364: 956–959.
10. Bao YL, Wang L, Pan HT, et al. Animal and organoid models of liver fibrosis. *Front Physiol* 2021; 12: 666138.
11. Prior N, Inacio P and Huch M. Liver organoids: from basic research to therapeutic applications. *Gut* 2019; 68: 2228–2237.
12. Brovold M, Keller D and Soker S. Differential fibrotic phenotypes of hepatic stellate cells within 3D liver organoids. *Biotechnol Bioeng* 2020; 117: 2516–2526.
13. Elbadawy M, Yamanaka M, Goto Y, et al. Efficacy of primary liver organoid culture from different stages of non-alcoholic steatohepatitis (NASH) mouse model. *Biomaterials* 2020; 237: 119823.
14. Leite SB, Roosens T, El Taghdouini A, et al. Novel human hepatic organoid model enables testing of drug-induced liver fibrosis in vitro. *Biomaterials* 2016; 78: 1–10.
15. Coll M, Perea L, Boon R, et al. Generation of hepatic stellate cells from human pluripotent stem cells enables in vitro modeling of liver fibrosis. *Cell Stem Cell* 2018; 23: 101–113.e7.
16. Ouchi R, Togo S, Kimura M, et al. Modeling steatohepatitis in humans with pluripotent stem cell-derived organoids. *Cell Metab* 2019; 30: 374–384.e6.
17. Salewskij K and Penninger JM. Blood vessel organoids for development and disease. *Circ Res* 2023; 132: 498–510.
18. Wang D, Wang E, Liu K, et al. Roles of TGFβ and FGF signals during growth and differentiation of mouse lens epithelial cell in vitro. *Sci Rep* 2017; 7: 7274.
19. Xu Y, Mu J, Zhou Z, et al. Expansion of mouse castration-resistant intermediate prostate stem cells in vitro. *Stem Cell Res Ther* 2022; 13: 299.
20. Song X, Yu Y, Leng Y, et al. Expanding tubular microvessels on stiff substrates with endothelial cells and pericytes from the same adult tissue. *J Tissue Eng* 2022; 13: 20417314221125310.
21. Yu Y, Leng Y, Song X, et al. Extracellular matrix stiffness regulates microvascular stability by controlling endothelial paracrine signaling to determine pericyte fate. *Arterioscler Thromb Vasc Biol* 2023; 43: 1887–1899.
22. Shen L, Song X, Xu Y, et al. Patterned vascularization in a directional ice-templated scaffold of decellularized matrix. *Eng Life Sci* 2021; 21: 683–692.
23. Hezode C, Castera L, Roudot-Thoraval F, et al. Liver stiffness diminishes with antiviral response in chronic hepatitis C. *Aliment Pharmacol Ther* 2011; 34: 656–663.
24. Friedrich-Rust M, Ong MF, Martens S, et al. Performance of transient elastography for the staging of liver fibrosis: a meta-analysis. *Gastroenterology* 2008; 134: 960–974.
25. Olsen AL, Bloomer SA, Chan EP, et al. Hepatic stellate cells require a stiff environment for myofibroblastic differentiation. *Am J Physiol Gastrointest Liver Physiol* 2011; 301: G110–G118.

26. Butcher DT, Alliston T and Weaver VM. A tense situation: forcing tumour progression. *Nat Rev Cancer* 2009; 9: 108–122.

27. Carvalho JR and Verdelho Machado M. New insights about albumin and liver disease. *Ann Hepatol* 2018; 17: 547–560.

28. Liang N, Yang T, Huang Q, et al. Mechanism of cancer stemness maintenance in human liver cancer. *Cell Death Dis* 2022; 13: 394.

29. Zhang Z, Wang Z, Liu T, et al. Exploring the role of ITGB6: fibrosis, cancer, and other diseases. *Apoptosis* 2024; 29: 570–585.

30. Zheng G, Bouamar H, Cserhati M, et al. Integrin alpha 6 is upregulated and drives hepatocellular carcinoma progression through integrin α6β4 complex. *Int J Cancer* 2022; 151: 930–943.

31. Duan X, Li H, Wang M, et al. PSMC2/ITGA6 axis plays critical role in the development and progression of hepatocellular carcinoma. *Cell Death Discov* 2021; 7: 217.

32. Ren D, Zhao J, Sun Y, et al. Overexpressed ITGA2 promotes malignant tumor aggression by up-regulating PD-L1 expression through the activation of the STAT3 signaling pathway. *J Exp Clin Cancer Res* 2019; 38: 485.

33. Adorno-Cruz V, Hoffmann AD, Liu X, et al. ITGA2 promotes expression of ACLY and CCND1 in enhancing breast cancer stemness and metastasis. *Genes Dis* 2021; 8: 493–508.

34. Guo P, Moses-Gardner A, Huang J, et al. ITGA2 as a potential nanotherapeutic target for glioblastoma. *Sci Rep* 2019; 9: 6195.

35. Affo S, Yu LX and Schwabe RF. The role of cancer-associated fibroblasts and fibrosis in liver cancer. *Ann Rev Pathol* 2017; 12: 153–186.

36. Zhang S, Wan Z and Kamm RD. Vascularized organoids on a chip: strategies for engineering organoids with functional vasculature. *Lab Chip* 2021; 21: 473–488.

37. Liu H, Zhang X, Liu J, et al. Vascularization of engineered organoids. *BMEMat* 2023; 1: e12031.

38. Wang D, Li LK, Dai T, et al. Adult stem cells in vascular remodeling. *Theranostics* 2018; 8: 815–829.

39. Ruwanpura SM, Thomas BJ and Bardin PG. Pirfenidone: molecular mechanisms and potential clinical applications in lung disease. *Am J Respir Cell Mol Biol* 2020; 62: 413–422.

40. Chastney MR, Conway JRW and Ivaska J. Integrin adhesion complexes. *Curr Biol* 2021; 31: R536–R542.

41. Slack RJ, Macdonald SJF, Roper JA, et al. Emerging therapeutic opportunities for integrin inhibitors. *Nat Rev Drug Discov* 2022; 21: 60–78.

42. Raghu G, Scholand MB, de Andrade J, et al. FG-3019 anti-connective tissue growth factor monoclonal antibody: results of an open-label clinical trial in idiopathic pulmonary fibrosis. *Eur Respir J* 2016; 47: 1481–1491.